

CYCLIC FATIGUE OF NITINOL

S. W. Robertson¹, J. Stankiewicz¹, X. Y. Gong², and R. O. Ritchie¹

¹ *Materials Sciences Division, Lawrence Berkeley National Laboratory, and Department of Materials Science and Engineering, University of California, Berkeley, CA 94720, USA*

² *Nitinol Devices & Components, 47533 Westinghouse Drive, Fremont, CA 94539, USA*

ABSTRACT

Nitinol's superelasticity, biocompatibility and magnetic resonance compatibility has led to its increasing popularity for the manufacture of endovascular stents. Despite its growing importance in the biomedical industry, especially under conditions involving pulsatile loading, the cyclic fatigue resistance of Nitinol is not well understood. This paper provides a summary of existing data on the fatigue-crack propagation properties of the superelastic alloy and presents preliminary results on crack-growth behavior in samples cut from Nitinol tube used as the starting material for the manufacture of endovascular stents. In addition, a new test sample for measuring the total fatigue life properties is described involving the uniaxial loading of slotted-tubular samples, again machined from Nitinol tube.

INTRODUCTION

Nitinol, a nearly equiatomic alloy of Ni and Ti, has many characteristics that make it favorable for use in endovascular stents, namely its superelasticity, biocompatibility, flexibility, and compatibility with magnetic resonance imaging (MRI) procedures. However, during handling and following deployment into the body, stents are subjected to cyclic stresses, *e.g.*, from the expansion and contraction of the blood vessels, which can result in fatigue damage and curtail their useful life. Despite the critical nature of this problem, the cyclic fatigue properties of Nitinol are not well understood. Much recent work on the fatigue of Nitinol has focused on determining the stress/strain-life (*S-N*) properties of wire and stent-like samples [1-10]. However, these measurements characterize the total life and do not reveal the individual contributions from the crack nucleation and crack growth stages. It is our contention that for a comprehensive understanding of the fatigue behavior of Nitinol, it is necessary to characterize these two stages

separately. However, data on fatigue-crack propagation in Nitinol are extremely limited. In fact, there have only been two previous studies that isolate crack-growth phenomena; both of which were performed on thick-section Nitinol product forms (40 mm diameter rod) that were not comparable to the thin sections used in current biomedical applications.

In the present work, we report the fatigue-crack propagation studies on product forms in superelastic Nitinol more relevant to those used for stents, *i.e.*, samples laser cut and flattened from 0.5 mm thick tubes and compare the results with the previous researches [11,12]. In addition, we present a method of determining total life fatigue data in Nitinol involving the *S-N* testing of slotted tubular samples, cut from 0.33 mm thick tube. These samples permit crack-length monitoring of incipient flaws, thereby enabling the separation of the nucleation and propagation life regimes.

EXPERIMENTAL PROCEDURES

Material

Nitinol fatigue samples, with a composition of 50.8 at% Ni were received from Nitinol Devices & Components, Inc. (Fremont, CA). Each sample was electropolished prior to testing to minimize surface discontinuities, and had an A_f temperature between 25° and 30°C. Two forms were used for the experiments conducted in this study:

Total life samples: 3.2 mm outer diameter, 0.33 mm wall thickness, 100 mm long tube with a 15 mm slot laser machined into the center (Fig. 1) to create a stress concentration in a specified gauge section of the sample.

Crack-propagation samples: ~12 mm square compact-tension C(T) specimens, laser cut and flattened from tubing with a wall thickness of ~0.5 mm (Fig. 2). The specimen dimensions were in accordance with ASTM E 647, which recommends testing with the same thickness configuration that is used in the final application of the material. The C(T) samples were cut either with the pre-crack running the circumference of the tube or with the pre-crack at a 45° angle to the circumference of the tube (Fig. 2). It is important to note that the only difference between these samples is their orientation relative to the axis of the tube; their processing was identical.



Fig. 1: Schematic diagram of slotted tube specimen used for uniaxial loading total-life fatigue studies; not to scale.

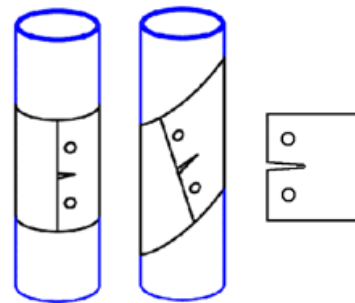


Fig. 2: Schematic diagram showing the two different orientations of the compact tension, C(T), samples and the resultant sample geometry after they were cut and flattened from the thin walled tube; not to scale.

Test Configuration

All fatigue tests were conducted on servo-hydraulic MTS mechanical testing systems with an enclosure around the sample and grips to maintain a temperature of 37°C in an air environment.

Total life (slotted tube) testing:

Testing was conducted in displacement control following an initial calibration of the load-line displacement with an MTS 9.15-mm extensometer. Uniaxial cyclic loading was performed at 50 Hz (sine wave) with a constant mean strain of 1.5% and variable alternating strains from 0.2 – 1.4%. It should be noted that this loading configuration was not intended to simulate *in vivo* conditions, but rather to provide a baseline for more relevant bend and torsional fatigue studies in the future. As heat treatments for stents vary from company to company, three heat treatments were chosen to enhance various microstructures but retain an A_f of $\sim 25^\circ\text{C}$ to study the possible effects of aging on the Nitinol tubing's fatigue characteristics and for comparison to concurrent studies [13,14]. The time and temperature and its expected changes in tubing microstructures are summarized below:

- 350°C, 37 min – increases grain size slightly from the as-drawn condition and enhances the R-phase. Transformation stress ~ 425 MPa.
- 500°C, 41 min – increases grain size further, causing annihilation of the nano-scale dislocation packets, lowers the stress plateau and transformation strain, but retains a nearly-fully-closed hysteresis loop.
- 500°C, 90 min – significantly increases grain size and Ni-rich precipitates, further lowers the stress plateau and transformation strain, and causes a residual strain following load removal (i.e., non-closed hysteresis loop).

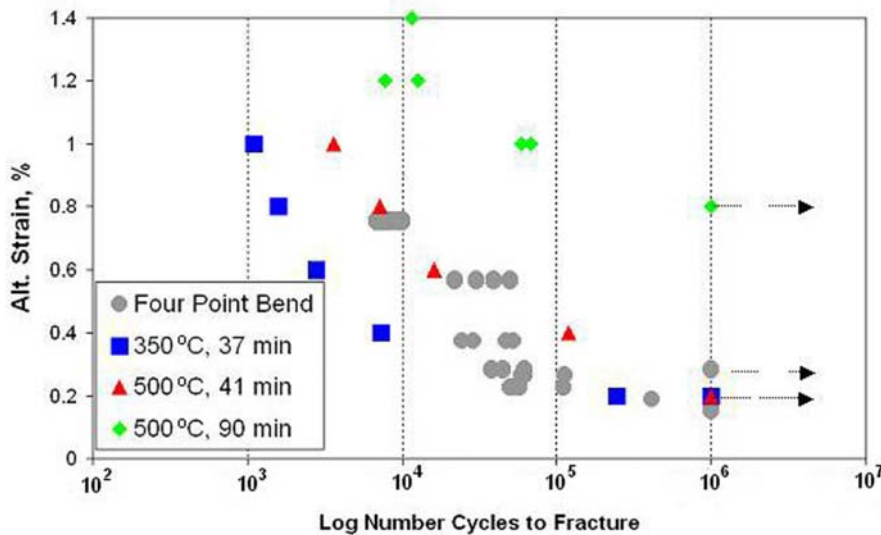


Fig. 3: Total fatigue life data for slotted tubes (red, blue, green) and four-point bend (gray) at a mean strain of 1.5% and variable alternating strains. All tests that went to 10^6 cycles were “run outs”, i.e., they did not fail.

Crack-propagation

C(T) testing:

Thin-walled flattened tube fatigue testing was performed in load control at a cyclic loading frequency of 50 Hz (sine wave) with load ratios (ratio of minimum to maximum load) of $R = 0.1$ and 0.5 ; crack lengths were continuously monitored with a load-line displacement gauge placed on the grips. Results are presented in the form of the crack-growth rates, da/dN , as a function of the

stress-intensity range, $\Delta K = K_{\max} - K_{\min}$, where K_{\max} and K_{\min} are, respectively, the maximum and minimum stress intensities in the loading cycle. Proprietary heat treatments were used during the C(T) flattening procedure which rendered the samples with an A_f of $\sim 30^\circ\text{C}$.

RESULTS AND DISCUSSION

Total Life, Slotted Tube Results

For S/N fatigue testing, a mean strain of 1.5% was chosen in order to compare the results with the available bend fatigue data [14] and because this strain represents the approximate transformation strain; as such, the alternating strains, even at low values, span both the pure austenitic elastic and the transforming regions. Results are shown in Fig. 3 and indicate a general trend of increasing fatigue life with increasing heat treatment time and temperature, perhaps due to the higher martensite volume at the same applied strain in the longer heat-treated samples. Samples heat-treated at 350°C and for shorter times at 500°C exhibited similar 10^6 cycle endurance strengths of $\sim 0.2\%$ alternating strain; however, longer annealing times at 500°C significantly raised the endurance strength to 0.8% alternating strain.

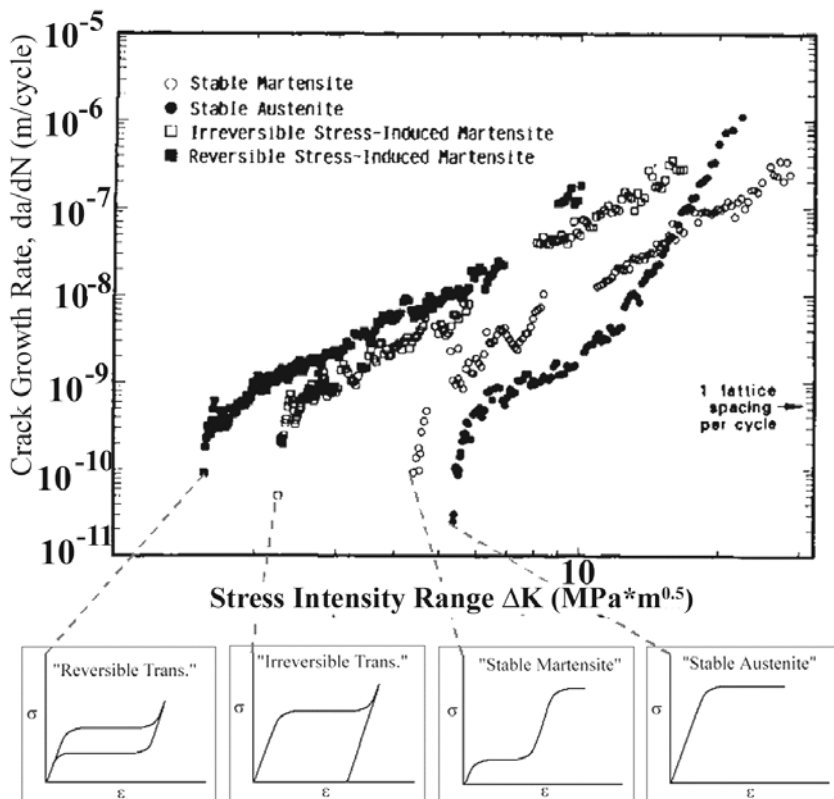


Fig. 4: Variation in fatigue-crack growth rates, da/dN , with the stress-intensity range, ΔK , for various phase structures. Tests were performed at a fixed temperature, at 37°C , with Nitinol of varying compositions chosen to vary the prevalent microstructural phase. Experiments involved 10 mm thick C(T) samples tested at a load ratio of $R = 0.1$ at a frequency of 50 Hz [11].

These results for the slotted tube geometry are similar to published fatigue life data for Nitinol in a completely different product form (0.8-mm diameter, electropolished wire; $A_f = 13^\circ\text{C}$) under different loading conditions (four-point bending) [14].

An advantage of using the slotted tube geometry, rather than the stent unit cell-like “diamond shaped” specimen, is that the surfaces can be conveniently replicated with silicone or acetate tape at specific logarithmic intervals throughout the test. This provides a means to characterize both the crack nucleation event(s) and to monitor the surface crack lengths during subsequent small

crack growth, thereby giving separate insight into the crack initiation and propagation stages. In this preliminary study where only limited replication was performed, scanning electron microscopy did reveal that the fatigue cracks initiated at the inner diameter of the tube. Work is currently in progress to use such replication techniques to study the mechanisms of crack initiation in Nitinol and to document the crack initiation lives.

Crack Propagation C(T) Results

As noted above, all previous studies on the fatigue-crack propagation behavior of Nitinol have been performed on thick-section material, specifically on 9-10 mm thick C(T) specimens machined from 40-mm diameter rod (Figs. 4-6) [11,12]. In addition to showing a marked, but expected, effect of load ratio on crack-growth rates (Fig. 6), these studies attempted to isolate the specific role of microstructure

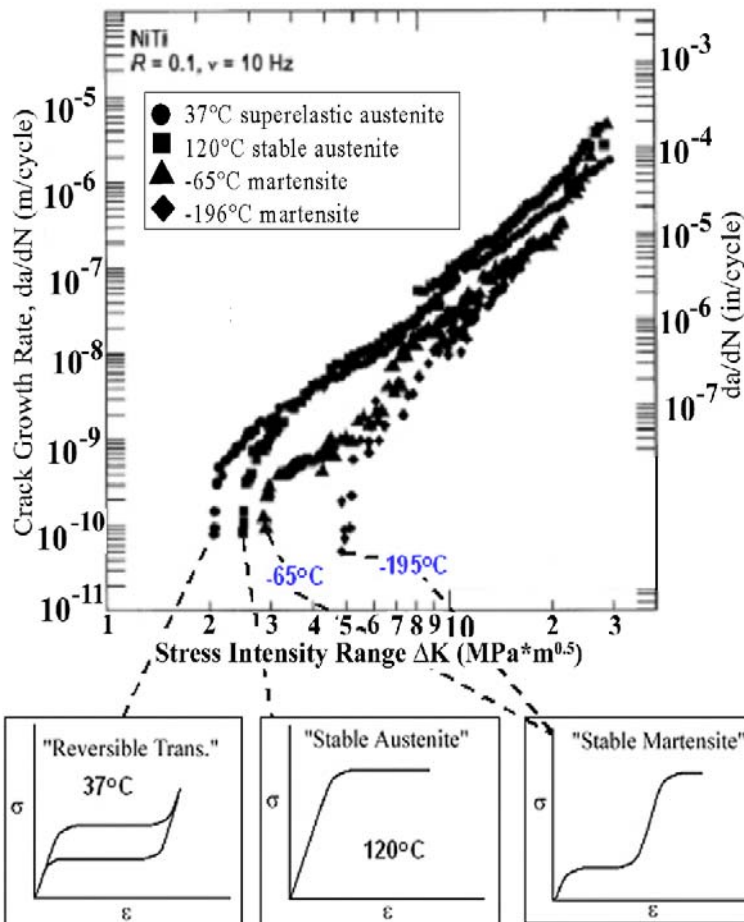


Fig. 5: Variation in fatigue-crack growth rates, da/dN , with the stress-intensity range, ΔK , for various phase structures. Tests were performed at a fixed Nitinol composition at various temps chosen to vary the prevalent phase. Experiments involved 9-mm thick C(T) samples tested at a load ratio of $R = 0.1$ at a frequency of 10 Hz [12].

and phase-transforming condition, *i.e.*, to discern the inherent fatigue-crack propagation resistance of stable austenite vs. superelastic austenite vs. stable martensite. This was achieved by testing (i) at a fixed temperature where the microstructural condition was changed by small compositional modifications (Fig. 4) [11], and (ii) at fixed alloy composition where the microstructural condition was changed by altering the testing temperature (Fig. 5) [12]. Both sets of experiments gave similar results; specifically, the martensitic structure was most resistant to fatigue-crack growth. In general, the non-transforming microstructures displayed far better fatigue-crack propagation resistance, *i.e.*, lower growth rates

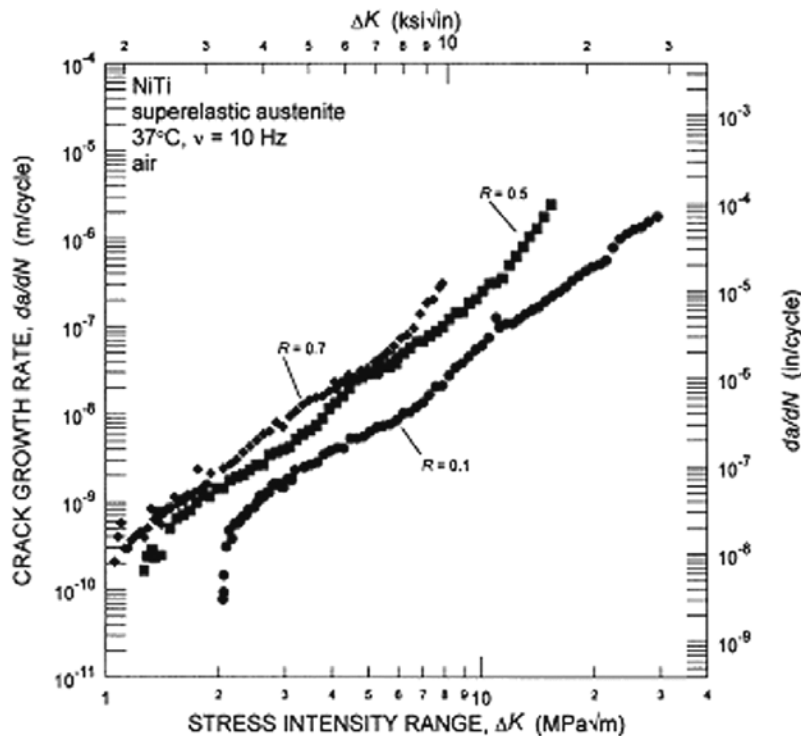


Fig. 6: Variation in fatigue-crack growth rates, da/dN , with the stress-intensity range, ΔK , as a function of load ratio (R varying from 0.1 to 0.7) for Nitinol with a superelastic austenite microstructure. Experiments involved 9-mm thick C(T) samples tested at 37°C at a frequency of 10 Hz [12].

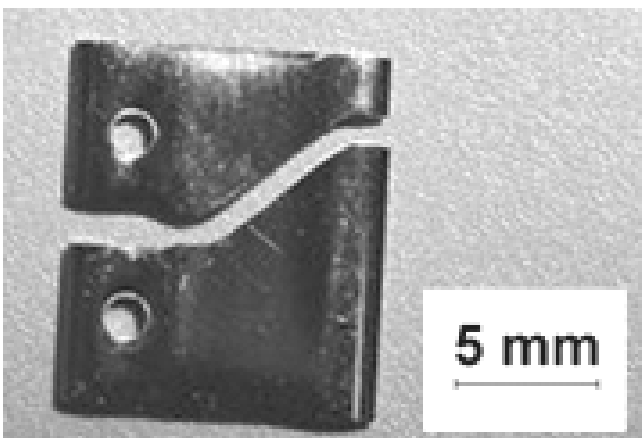


Fig. 7: Circumferentially-oriented thin-walled tube C(T) specimen with a 45° deflected crack path trajectory due to texture.

and higher ΔK_{th} fatigue threshold values, than the transforming (superelastic) structures. The apparent low fatigue-crack growth resistance of the superelastic structures is believed to be associated with the fact that stress-induced austenite-to-martensite transformation involves a small negative dilation ($\sim 0.5\%$) in Nitinol. When this transformed region is confined to a small zone at the crack tip and is therefore constrained by surrounding non-transforming material, the effect is to induce additional tensile stresses at the crack tip [15], thereby promoting crack growth. This is the analogous, yet opposite, effect to the well-known mechanism of transformation-toughening in zirconia ceramics, where the positive dilation associated with the transformation imparts compressive stresses at the tip, thereby toughening the material [16].

The current interests in the fatigue-crack propagation resistance of Nitinol are focused on testing sample geometries more appropriate to biomedical stent applications, specifically C(T) specimens machined from flattened 0.5-mm thick Nitinol tube. However, initial specimens cut circumferentially from the tube produced 45-degree deflected cracks (Fig. 7), a phenomenon that was attributed to texture yet was only observed in fatigue (see ref. [17]). From the perspective of

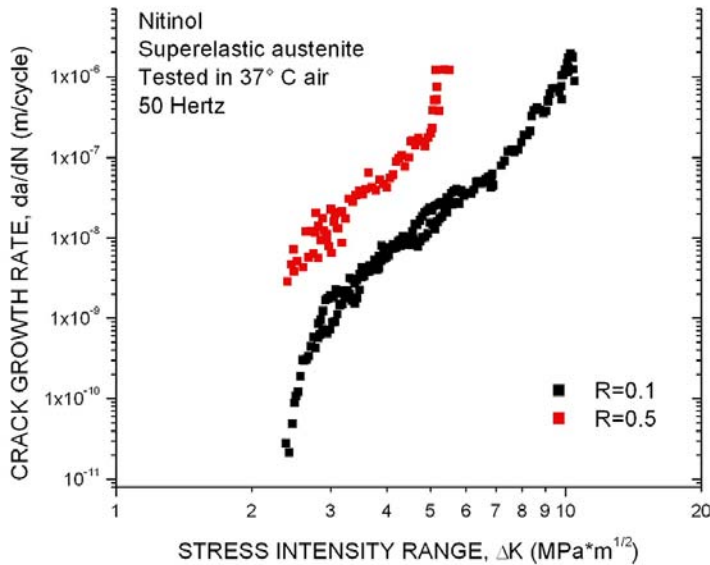


Fig. 8: Fatigue-crack growth data at varying load ratio in thin-walled superelastic Nitinol tube showing higher crack growth rates at higher R ratios. Tests in air at 37°C at a frequency of 50 Hz.

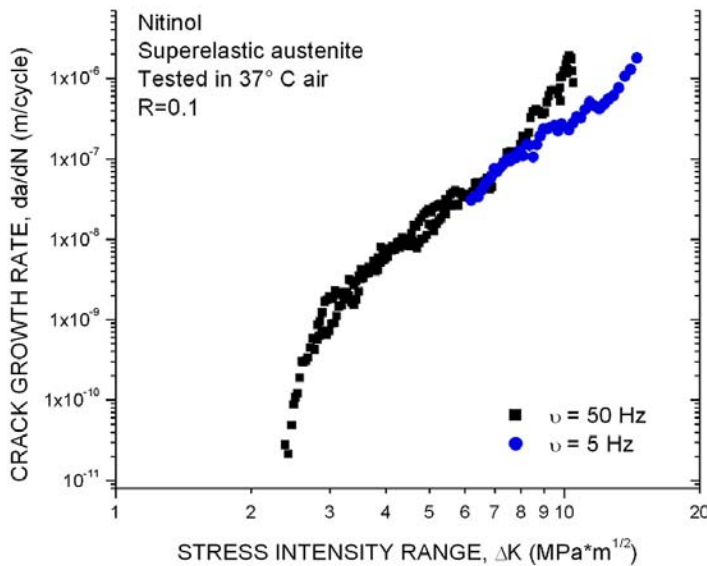


Fig. 9: Fatigue-crack growth of varying frequency in thin-walled superelastic Nitinol tube showing essentially frequency-insensitive behavior (except at very high growth rates close to final fracture). Tests in air at 37°C at frequencies of 5 and 50 Hz.

being able to reliably measure crack-growth rate behavior, this “problem” was solved by rotating the C(T) specimen orientation in the tube (see Fig. 2), which led to non-deflecting Mode I crack trajectories.

The results of these fatigue-crack propagation tests on the “rotated” C(T) specimens are presented in Figs. 8-10, and indicate preliminary data on the effect of load ratio, test frequency, and heat treatment/product form. With respect to load ratio, as with the thick-section Nitinol studied by McKelvey and Ritchie [12], increasing the load ratio, in this instance from 0.1 to 0.5, led to faster crack growth rates and expected lower ΔK_{th} threshold values (Fig. 8).

With respect to test frequency, limited results to date have examined the effects of lowering the frequency one logarithmic unit from 50 to 5 Hz. As shown in Fig. 9, little effect of frequency can be seen, although growth rates do appear to be faster at the higher frequency as instability is approached.

Perhaps the most interesting phenomenon was the effect of heat treatment on the fatigue-crack propagation behavior, shown in Fig 10. A heat treatment of 850°C for 30 min was chosen because it produces a very similar texture to the as-drawn and flattened tube [18].

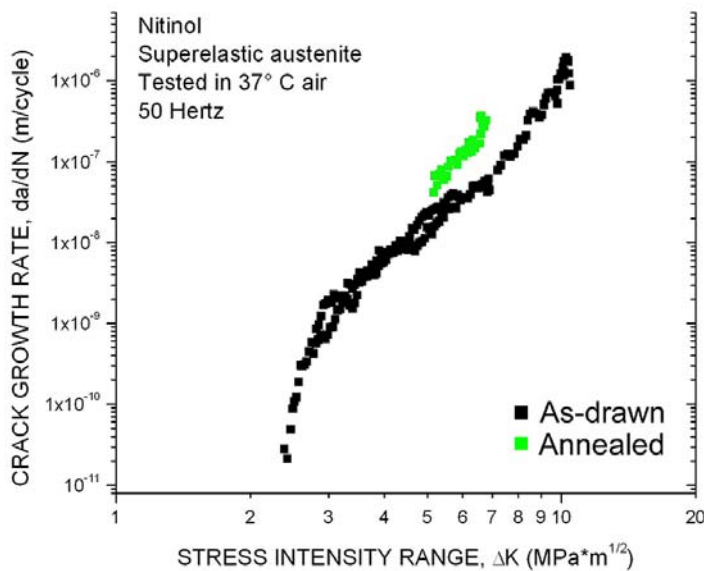


Fig. 10: Effect of annealing (850°C , 30 min, slow cool $10^{\circ}\text{C}/\text{min}$) on fatigue-crack growth behavior in thin-walled Nitinol tube showing increased crack-growth rates in the annealed compared to the as-drawn samples. Tests in air at 37°C at a frequency of 50 Hz.

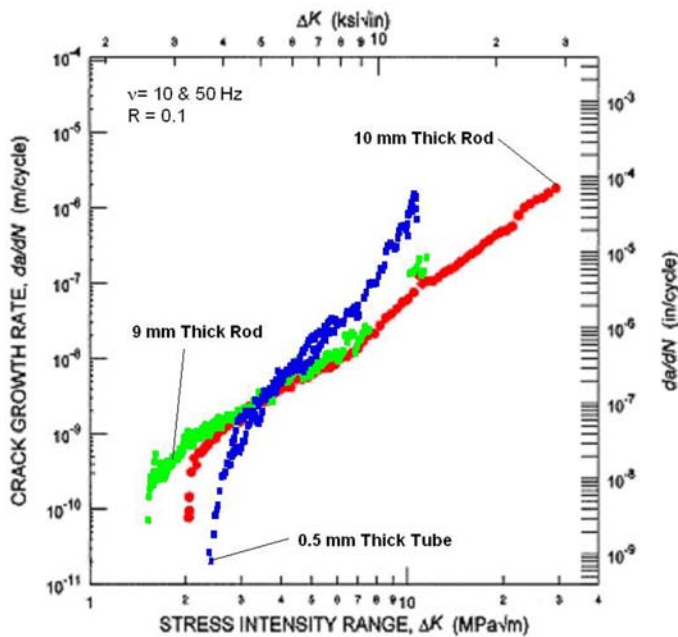


Fig. 11: Comparison of the fatigue-crack propagation behavior of Nitinol in various product forms: thick-section (9-10 mm thick, \varnothing 40 mm) Nitinol and thin-section (0.5-mm thin-walled tube) Nitinol.

Annealing at the higher temperature for greater length of time produced faster fatigue-crack growth rates in the thin-walled tube. This trend was the opposite of that observed fatigue-life experiments presented in Fig. 3, and is a good example where the effect of a variable such as heat treatment or microstructure on crack-propagation behavior is quite different to its effect on crack initiation, thereby reinforcing the need to isolate the initiation and growth stages in experimental studies focused on understanding the fatigue behavior of Nitinol.

Fig. 11 compares the results of our previous studies of fatigue-crack propagation behavior in thick-section (9-10 mm thick) Nitinol with the current preliminary results on thin-section tubular Nitinol. It is apparent that superelastic thin-section Nitinol does appear to be superior to the thick-section material in the all-important low growth-rate regime. This effect may be associated with the fact that in a thin sections, the constraint of surrounding untransformed material on the crack-tip transformation zone may be minimal, thereby limiting the creation of additional (transformation-induced tensile) stresses at the crack tip.

SUMMARY

It is not the purpose of this paper to conclude which approach to fatigue, *i.e.*, total-life vs. crack propagation, is most appropriate for the design and life-prediction of Nitinol biomedical implants such as stents,

but rather to emphasize that to fully understand cyclic fatigue in this complex material, it is necessary to discern their separate contributions to the fatigue life. In light of this, we have presented preliminary results on both stages using thin-section superelastic Nitinol samples relevant to endovascular stent components, namely total-life testing on a slotted tube geometry where monitoring the characteristics of crack nucleation is feasible using replication, and crack-propagation studies on compact-tension samples machined from flattened Nitinol tubes.

Preliminary total-fatigue life studies on uniaxially-loaded slotted tubes (with 1.5% mean strain) of superelastic Nitinol ($A_f \sim 25^\circ\text{C}$) revealed that increasing the annealing time and temperature resulted in improved fatigue lifetimes. Specifically, annealing at 500°C for 90 min produced a 10^6 -cycle endurance strength of $\sim 0.8\%$ alternating strain, compared to an endurance strength of only $\sim 0.2\%$ after shorter annealing treatments at 350°C (for 37 min) and at 500°C (for 41 min), an effect possibly due to the higher martensite volume fractions in the samples with longer annealing times.

In addition to summarizing the available information in the literature on fatigue-crack propagation in Nitinol, which is confined to thick-section material, we have also presented preliminary results on the crack-growth behavior in the thin-walled tubes. In general, it is found that the orientation of the samples can lead to significant change in properties, specifically in crack trajectories, due to the influence of texture. Indeed, a preferred fatigue crack path of 45° , i.e., spirally within the tube wall, was observed. However, for cracks oriented in normal Mode I loading, fatigue threshold ΔK_{th} values of $\sim 2.2 \text{ MPa}\sqrt{\text{m}}$ were found in the thin-section superelastic Nitinol, which is between 10 to 50% higher than thresholds measured previously in thick-section material [11,12], but still lower than other implantable bioengineering metallic alloys, where thresholds typically exceed $3.5 \text{ MPa}\sqrt{\text{m}}$ [19]. Despite its excellent fatigue resistance under strain-controlled loading, Nitinol's low resistance to fatigue-crack propagation under stress-control is believed to be associated with the presence of tensile stresses developed at the crack tip due to the formation of a constrained transformation zone. We surmise that in very thin sections, such as in a stent, this constraint may be minimal, thereby limiting the generation of the transformation-induced tensile stresses. Although this explanation remains to be proven, it does provide a feasible mechanism as to why the near-threshold fatigue-crack propagation resistance of superelastic Nitinol is superior in thin sections.

ACKNOWLEDGMENTS

This work was supported by a gift from Nitinol Devices and Components (NDC), Inc., Fremont, California to the University of California at Berkeley and from the National Science Foundation (Grant Number CMS-0409294). Thanks are due to Drs. Tom Duerig and Alan Pelton of NDC for their financial support, supply of Nitinol samples, and for many helpful discussions, and to Tracy Lopes, Christine Trepanier, and Dung Pham of NDC for producing the test samples.

REFERENCES

- [1] W.J. Harrison, Z.C. Lin, *Proc. of the Int. Conf. on Shape Memory and Superelastic Technologies.*, SMST Society, Inc., Menlo Park, CA, 2000, pp. 391-396.
- [2] D. Tolomeo, S. Davidson, M. Santinoranont, *Proc. of the Int. Conf. on Shape Memory and Superelastic Technologies*, SMST Society, Inc., Menlo Park, CA, 2000, pp. 471-476.
- [3] D. Wurzel, E. Hornbogen, *Proc. of the Int. Conf. on Shape Memory and Superelastic Technologies*, SMST Society, Inc., Menlo Park, CA, 2000, pp. 383-390.

- [4] A.R. Pelton, J. DiCello, S. Miyazaki, *Proc. of the Int. Conf. on Shape Memory and Superelastic Technologies*, SMST Society, Inc., Menlo Park, CA, 2000, pp. 361-374.
- [5] A.R. Pelton, X.Y. Gong, T.W. Duerig, *Proc. of the Int. Conf. on Shape Memory and Superelastic Technologies*, SMST Society, Inc., Menlo Park, CA, 2003, pp. 293-302.
- [6] N.B. Morgan, J. Painter, A. Moffat, *Proc. of the Int. Conf. on Shape Memory and Superelastic Technologies*, SMST Society, Inc., Menlo Park, CA, 2003, pp. 303-310.
- [7] G. Eggeler, E. Hornbogen, A. Yawny, A. Heckmann, M. Wagner, *Mater. Sci. Eng. A*, vol. 378, 2004, pp. 24-33
- [8] M. Wagner, T. Sawaguchi, G. Kausträter, D. Höffken, G. Eggeler, *Mater. Sci. Eng. A*, vol. 378, 2004, pp. 105-109
- [9] O. Prymak, A. Klocke, B. Kahl-Nieke, M. Epple, *Mater. Sci. Eng. A*, vol. A378, 2004, pp. 110-114
- [10] D. Fife, G. Gambarini, L.R. Britto, *Oral Surgery, Oral Medicine, Oral Pathology, Oral Radiology & Endodontics*, vol. 97, 2004, pp. 251-256
- [11] R.H. Dauskardt, T.W. Duerig, R.O. Ritchie, in K. Otsuka and K. Shimitsu, eds., *Shape Memory Alloys*, Proc. MRS International Meeting on Advanced Materials, vol. 9, pp. 243-249, Materials Research Society, Pittsburgh, PA, 1989.
- [12] A.L. McKelvey, R.O. Ritchie, *Metall. Mater. Trans. A*, vol. 32A, 2001, pp. 731-743.
- [13] X. Gong, T. Lopes, C. Trepanier, oral presentation at the *ASM Materials & Processes for Medical Devices Conference*, St. Paul, MN, USA, August 2004.
- [14] A. Wick, X.Y. Gong, C. Trepanier, A. Pelton, in *SMST-2004, Proc. of the Int. Conf. on Shape Memory and Superelastic Technologies*, SMST Society, Inc., Menlo Park, CA, 2004.
- [15] W. Yan, C.H. Wang, X.P. Zhang, Y.W. Mai, *Mater. Sci. Eng. A*, vol. A354, 2003, pp. 146-157.
- [16] A.G. Evans, *J. Am. Ceram. Soc.*, vol. 73, 1990, pp. 187-206.
- [17] J. Stankiewicz, S.W. Robertson, X.Y. Gong, H.R. Wenk, R.O. Ritchie, in *Proceedings of the 2004 SEM Annual Conference*, Costa Mesa, CA, Society for Experimental Mechanics, Bethel, CN, 2004.
- [18] S.W. Robertson, V. Imbeni, H.R. Wenk, R.O. Ritchie, in *SMST-2004, Proc. of the Int. Conf. on Shape Memory and Superelastic Technologies*, SMST Society, Inc., Menlo Park, CA, 2004.
- [19] A.L. McKelvey, R.O. Ritchie, *J. Biomed. Mater. Res.*, vol. 47, 1999, pp. 301-308.